

25. P. Kurada and J. E. O'Tousa, *Neuron* **14**, 571 (1995).
26. Such mutations include dominant mutations of rhodopsin (25) and mutations on the receptor-specific cyclophilin *ninaA* that reduce rhodopsin amounts to $\leq 10\%$ those of wild-type flies (J. Vinós and C. Zuker, unpublished data).
27. K. Scott, A. Becker, Y. Sun, R. Hardy, C. Zuker, *Neuron* **15**, 919 (1995).
28. Z. Selinger, Y. Doza, B. Minke, *Biochim. Biophys. Acta* **1179**, 283 (1993).
29. J. Chen, C. L. Makino, N. S. Peachey, D. A. Baylor, M. I. Simon, *Science* **267**, 374 (1995).
30. J. L. Benovic *et al.*, *Proc. Natl. Acad. Sci. U.S.A.* **84**, 8879 (1987); R. J. Lefkowitz *et al.*, *Cold Spring Harbor Symp. Quant. Biol.* **57**, 127 (1992).
31. W. C. Smith *et al.*, *J. Biol. Chem.* **269**, 15407 (1994).
32. W. L. Pak, in *Neurogenetics: Genetic Approaches to the Nervous System*, X. O. Breakfield, Ed. (Elsevier, New York, 1979), pp. 67–99.
33. T. J. Keen *et al.*, *Genomics* **11**, 199 (1991).
34. T. Li, W. K. Franson, J. W. Gordon, E. L. Berson, T. P. Dryja, *Proc. Natl. Acad. Sci. U.S.A.* **92**, 3551 (1995).
35. J. Rim and D. D. Oprian, *Biochemistry* **34**, 11938 (1995).
36. E. Montini *et al.*, *Hum. Mol. Genet.* **6**, 1137 (1997).
37. Flies used in the phosphorylation, degeneration, and electrophysiology experiments were 4 days old and were raised and kept in the dark. The following stocks were used: w^1 , w^{1118} , $w^{1118};ninaE^{234}$, $w^{1118};rdgC^{306}cu\ red$, $w^{1118};P[ninaE^{\Delta 356}ry^+]ry\ ninaE^{117}e^s$ ($Rh1\Delta 356$), $w^{1118};P[ninaE^{\Delta 356}ry^+];rdgC^{306}cu\ red\ ry\ ninaE^{117}e^s$ ($Rh1\Delta 356;rdgC$), $w^{1118};Dgq^1\ cn$, $w^{1118};Dgq^1\ cn;rdgC^{306}cu\ red$, and $w^{1118};Arr2^3$. In phosphorylation experiments, the amount of label ingested was monitored by adding a green food dye to the radioactive food. For each sample, 10 flies were subjected to 4 hours of starvation in the dark and were then transferred to a vial containing 50 μ l of 1% sucrose, 0.5% agarose, and 50 μ Ci of carrier-free $^{32}PO_4$. Flies were kept in a dark, humid chamber overnight and were then exposed to either 20 s or 15 min of blue or orange light. Light exposure times were selected to maximize differences between phenotypes. Flies were then frozen in liquid nitrogen and dried in cold acetone for 3 hours at $-80^\circ C$ followed by 16 hours at $-20^\circ C$. Retinas were hand-dissected and homogenized in electrophoresis sample buffer containing the phosphatase inhibitors okadaic acid and microcystin. Proteins were separated by denaturing electrophoresis, blotted to nitrocellulose, analyzed on a phosphorimager, and then probed with specific antibodies.
38. For microscopy, flies (37) were exposed to white light (30-W white lamp, attenuated 1:100, at 15 cm) for 6 days. Fly heads were cut, fixed, and embedded in resin as described [D. P. Smith *et al.*, *Science* **254**, 1478 (1991)]. Sections (1 μ m thick) were stained with methylene blue and borax before analysis.
39. J. Vinós, R. Hardy, C. Zuker, unpublished data.
40. ERGs of 4-day-old adult, dark-raised flies were recorded as described (32). Stimulating light was delivered with a 450-W xenon lamp (Osram) and filtered with either a 480-nm bandpass filter (Oriel, 53850) for blue light or a 570-nm longpass filter (Oriel, 51310) for orange light. Recordings (Fig. 3A) were performed with orange light attenuated 1:1585. Similar responses were elicited with blue light. For intracellular recordings, a coronal section was made through the compound eye. Dorsal hemispheres of the head were mounted upside down and immediately immersed in Schneider's medium (Gibco). Photoreceptor cells were impaled with 90- to 150-M Ω electrodes filled with 2 M KCl. Maximal differences in deactivation time were found when stimuli 0.5 s or longer were used. Under whole-cell recording conditions, no significant differences in deactivation time were found.
41. We thank P. Dolph for suggestions and fly stocks, and A. Newton and members of the Zuker laboratory for critical reading of the manuscript. K.J. is an American Cancer Society junior fellow, R.W.H. is an associate of the Howard Hughes Medical Institute, and C.S.Z. is an investigator of the Howard Hughes Medical Institute. Supported in part by a grant from the National Eye Institute.

31 March 1997; accepted 18 June 1997

Simplification of DNA Topology Below Equilibrium Values by Type II Topoisomerases

Valentin V. Rybenkov, Christian Ullsperger,
Alexander V. Vologodskii, Nicholas R. Cozzarelli*

Type II DNA topoisomerases catalyze the interconversion of DNA topoisomers by transporting one DNA segment through another. The steady-state fraction of knotted or catenated DNA molecules produced by prokaryotic and eukaryotic type II topoisomerases was found to be as much as 80 times lower than at thermodynamic equilibrium. These enzymes also yielded a tighter distribution of linking number topoisomers than at equilibrium. Thus, topoisomerases do not merely catalyze passage of randomly juxtaposed DNA segments but control a global property of DNA, its topology. The results imply that type II topoisomerases use the energy of adenosine triphosphate hydrolysis to preferentially remove the topological links that provide barriers to DNA segregation.

Randomly cyclized DNA molecules can be found in three topological forms (1): supercoils, knots, and catenanes (Fig. 1). If cyclization is sufficiently slow, the distribution of topological isoforms of circular DNA will be at thermodynamic equilibrium. This equilibrium distribution depends solely on the conformations adopted by DNA during its thermal fluctuations in solution (2, 3). The study of topological equilibrium has provided valuable information about DNA superhelical energy (4, 5), DNA effective diameter (6), and the conformations of supercoiled DNA (3).

A widely held belief is that, with the obvious exception of DNA gyrase and reverse gyrase, which introduce supercoiling in circular DNA (7), topological equilibrium is also achieved in the reactions catalyzed by DNA topoisomerases. Accordingly, topoisomerases were described as enzymes that convert a real DNA chain into a phantom chain that freely passes through itself to generate the equilibrium set of topological isomers. In support of this view, a mouse type I topoisomerase (topo I) generated the same Gaussian distribution of linking number (Lk) topoisomers as did ligation of a nicked circular DNA (5). Type II topoisomerases (topo II) can also relax supercoiled DNA. They can unlink knotted (8, 9) or catenated DNA (10, 11) and promote catenation if the DNA concentration is high enough (11). In all these reactions, the systems approach equilibrium. However,

the question of whether the enzymes create an equilibrium distribution of relaxed, catenated, or knotted molecules has not been carefully examined.

Our previous studies of equilibrium DNA conformations (3, 6) provided the tools to determine whether the product distributions of the reactions catalyzed by prokaryotic and eukaryotic type II topoisomerases matched those at equilibrium. First, we measured the equilibrium fraction of catenanes between two nicked circular DNA molecules (3, 6). Bacteriophage P4 DNA (2 μ g/ml) was cyclized by means of its long cohesive ends in the presence of excess (50 μ g/ml) nicked plasmid pAB4 DNA, and the fraction of heterodimeric catenanes among all cyclized molecules was measured. More than 90% of the catenanes were singly linked dimers. The probability of catenation was proportional to the concentration of pAB4 DNA. Previous experimental data strongly support the conclusion that cyclization of DNA by its cohesive ends results in an equilibrium distribution of topological species, and this was confirmed by Monte Carlo simulations (2, 3).

To measure the fraction of catenanes in a topoisomerase-catalyzed reaction, we used the same mixture of pAB4 and P4 DNA molecules as a substrate but with twice the equilibrium fraction of catenanes (12). The fraction of catenanes as a function of the amount of *Escherichia coli* topoisomerase IV was measured by agarose gel electrophoresis (Fig. 2A). This fraction decreased to 0.004 when the molar ratio of enzyme to DNA, s , was 0.1 to 1 (Fig. 2B). Over this range of s , we found the same fraction of catenanes in the reverse reac-

V. V. Rybenkov, C. Ullsperger, N. R. Cozzarelli, Department of Molecular and Cell Biology, University of California, Berkeley, CA 94720, USA.

A. V. Vologodskii, Department of Chemistry, New York University, New York, NY 10003, USA.

*To whom correspondence should be addressed. E-mail: cozzlab@mendel.berkeley.edu

tion, in which the substrate was a completely unlinked mixture of circular P4 and pAB4 DNA (Fig. 2B). In both the forward and reverse reactions, the fraction of catenanes did not change with in-

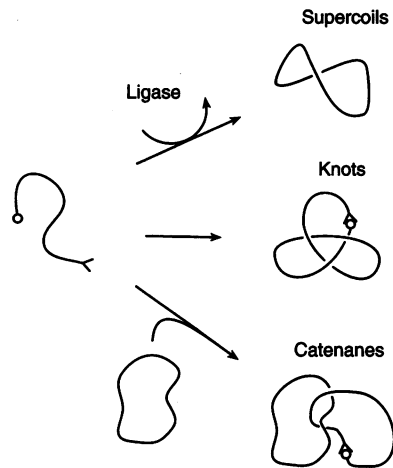


Fig. 1. Generation of topological equilibria in circular DNA. During the random cyclization of a linear duplex DNA with cohesive ends (circle and caret), a population of numerous topologically distinct species is formed. The relative abundance of these species, which may be knotted, catenated, or, after ligation of the nicks, supercoiled, is defined entirely by the conformations of circular DNA in solution. The equilibrium distribution obtained is the same as that produced by free strand passage of corresponding phantom polymer chains.

creased reaction time. Hence, the reaction reached its steady state at these values of s . We use the term “steady state” to acknowledge the continuous adenosine triphosphate (ATP) hydrolysis in the enzymatic reaction and to distinguish it from thermodynamic equilibrium. The steady-state fraction of catenanes was 16 times lower than the value at topological equilibrium. Because the reaction reached the steady state at substoichiometric enzyme to DNA ratios, the lower fraction of catenanes reflected the mechanism of the topoisomerase rather than distortion of DNA conformations caused by the binding of several enzyme molecules. In fact, the binding of several enzyme molecules to DNA resulted in an increase in the complexity of the products (see Fig. 2 for $s \geq 1$), as has been shown previously for knotting (8).

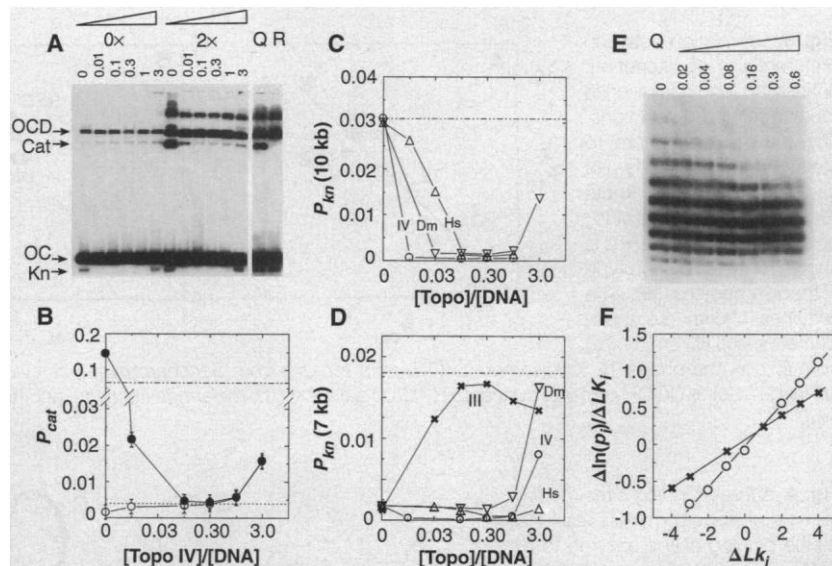
After treatment with topo IV, the fraction of knotted DNA molecules was reduced even more (Fig. 2, A and C). Under these reaction conditions, 3.1% of nonenzymatically cyclized P4 DNA are trefoil knots (6). After treatment of the equilibrium mixture with topo IV, the fraction of trefoils decreased by more than a factor of 50 (Fig. 2C). Similarly, the steady-state fraction of knots in pAB4 DNA treated with topo IV was more than 90 times lower than the corresponding equilibrium value (Fig. 2D).

We also studied the Lk distribution generated by topo IV in pAB4 DNA. The variance of the distribution $\langle \Delta Lk^2 \rangle$ was 1.7, a 1.8 times decrease compared with its equilibrium value, 3.1 (Fig. 2, E and F). Thus, the deviations from equilibrium for the topo IV-catalyzed reactions involved all aspects of topological equilibrium in circular DNA.

Topoisomerases from bacteriophage, yeast, *Drosophila melanogaster*, and human cells were also tested. Some of the data for unknotting as a function of s are shown in Fig. 2, C and D. All the results are summarized in Fig. 3 in terms of R , the ratio of the equilibrium fraction of catenanes, knots, or $\langle \Delta Lk^2 \rangle$ to those at the enzymatic steady state. All five type II topoisomerases tested reduced the fraction of catenanes and knots, and narrowed the Lk distribution in DNA compared with the equilibrium level. Although the magnitude of the effect varied among the topoisomerases, there was a strong correlation between the steady-state fractions of catenanes, knots, and $\langle \Delta Lk^2 \rangle$ found for each enzyme (Fig. 3). Thus, a highly conserved mechanistic feature of type II topoisomerases seems to be responsible for preferential removal of all topological links from DNA.

For all cases, the reaction was complete at substoichiometric amounts of enzyme. The free energy required to simplify DNA topology must be provided by ATP hydroly-

Fig. 2. Type II topoisomerases remove topological links from DNA to levels below equilibrium. **(A)** Gel electrophoresis analysis of DNA decatenation by topoisomerase IV from *E. coli*. Mixtures containing either no heterodimeric catenanes (0x) of bacteriophage P4 and plasmid pAB4 DNA circles, or twice the equilibrium amount of these catenanes (2x) were treated with increasing amounts of topoisomerase (12), and the DNA products were resolved by gel electrophoresis. The DNA was visualized by Southern (DNA) blotting with P4 DNA as a probe, then quantified with a Phosphorimager. The enzyme to DNA molar ratio, s , is indicated above each lane. The arrows on the left indicate positions of topological isoforms of P4 DNA circles: uncatenated unknotted (OC), uncatenated but knotted (Kn), and catenated with pAB4 DNA (Cat); OCD, dimeric circular P4 DNA. Controls: lane Q, P4 DNA nonenzymatically cyclized in the presence of pAB4 DNA, which contains catenanes and knots at their equilibrium levels; lane R, DNA from lane Q cut with Eco O109 restriction endonuclease, which cleaves pAB4 but not P4 DNA. **(B)** Quantitative analysis of the gel shown in (A). The final fraction of catenated P4 DNA molecules (P_{cat}) after reaction with 0x (○) or 2x (●) catenane concentrations is plotted as a function of the topoisomerase to DNA molar ratio, s . Except for the no-enzyme point, the values of s are shown on a logarithmic scale. The reaction reached its steady state (dotted line) at substoichiometric values of s . The equilibrium fraction of catenanes is shown with an intermittent dashed line. Unknotting of 10-kb P4 DNA **(C)** and 7-kb pAB4 DNA **(D)** by type II topoisomerases. The extent of knotting is shown for topo IV (○), *Drosophila* topo II (▽), and human topo II α (△). Also shown are the fractions of knots found for topo III, a type I topoisomerase from *E. coli* with an efficient decatenation activity (x). The equilibrium fractions of knots in P4 and pAB4 DNA are indicated by intermittent dashed lines. **(E)** Nonequilibrium removal of supercoils from circular



DNA. Plasmid pAB4 was relaxed to equilibrium with wheat germ topo I under standard topo IV assay conditions (lane Q). We treated 125 fmol of this relaxed DNA for 20 min with topo IV (12); the stoichiometric ratio, s , is indicated above each lane. **(F)** Linear transformation of Lk topoisomer distributions from (E) generated by topo I (○) and 40 fmol topo IV (x) (4). The slopes of the lines correspond to the variance of the distribution, $\langle \Delta Lk^2 \rangle$. ΔLk_i is the linking number of a topoisomer relative to that of a reference topoisomer close to the center of the distribution; p_i is the amount of a given topoisomer.

ysis. Type I topoisomerases, except for reverse gyrase, do not use high-energy cofactors in their reactions (7). Therefore, in compliance with the second law of thermodynamics, the topological distributions in reactions with type I topoisomerases must approach thermal equilibrium. Indeed, we found that topo III from *E. coli* (7), a type I topoisomerase which can change the topology of nicked or gapped DNA circles, generates the equilibrium amounts of catenanes ($R_{cat} = 1.2$) and knots ($R_{kn} = 1.1$) (Fig. 3A). We also observed the equilibrium distribution of Lk for wheat germ topo I ($R_{Lk} = 1.0$), as was found before with mouse topo I (5).

Whereas ATP hydrolysis allows type II topoisomerases to remove topological links from DNA below their equilibrium values, how this is achieved mechanistically remains a puzzle. Free strand passage during the thermal motion of circular DNA molecules should establish an equilibrium distribution of topological forms. This distribution would not change even if only a fraction of the segment collisions results in strand passage, as long as the probability of passage is independent of DNA topology. We conclude that the enzymes not only transport DNA segments through each other but also assess DNA topology during the reaction.

However, a single topoisomerase, given its small size compared to DNA, cannot recognize the topological state of DNA by

binding the whole molecule. The topoisomerase must use local interactions with DNA to affect DNA topology. Local interactions, however, provide only limited information about DNA topology. The only property of randomly colliding DNA segments that a topoisomerase might conceivably exploit to simplify DNA topological distributions is the angle in the crossing of the two segments. In the decatenation reaction, for example, a topoisomerase could catalyze strand passage for the angles that are favored in catenated as opposed to unlinked DNA molecules (13, 14). However, Monte Carlo simulations show that the probability of any angle between juxtaposed segments of catenated rings deviates from that of unlinked rings by less than 20% (15). This difference cannot provide the observed reduction of 16 times in the fraction of catenanes by topo IV.

A plausible but unproven explanation of our results is that type II topoisomerases effectively shorten the DNA during the course of their reaction. The probability of knots and catenanes and the value of $\langle \Delta Lk^2 \rangle$ decrease with decreasing DNA length (3–6). Therefore, if the DNA is effectively shortened, the steady-state fractions of knots and catenanes and the value of $\langle \Delta Lk^2 \rangle$ would be lower than the equilibrium values (16).

The effective DNA length would be reduced if several DNA segments are bound simultaneously by the enzyme. For example,

topoisomerases could bind cooperatively to the same DNA molecule to bring multiple DNA segments together (17). However, measurements of DNA binding and the rate of ATP hydrolysis by yeast topo II did not reveal any cooperativity in the interactions of topo II with DNA (13, 18, 19). Furthermore, at stoichiometric amounts of topo II ($s > 1$), we observed an increase rather than a decrease in the fraction of topologically complex DNA forms (Fig. 2). Thus, it is more likely that a single topoisomerase molecule simultaneously binds to several DNA segments.

We propose as a working model that a single type II topoisomerase molecule binds three DNA segments. The topoisomerase forms an intermediate complex with two noncontiguous DNA segments (Fig. 4). The existence of such a crossover complex is supported by electron microscopic and biochemical studies that have shown that type II topoisomerases bind preferentially to DNA crossovers (19, 20). Only one of the two crossover segments, however, has a previously assigned function: in the nomenclature of Roca and Wang (21), it is the gate segment (G-segment) which is cleaved and religated during strand passage. We propose that the segment that is transported (T-segment) through the gate does not constitute a part of the crossover complex (22). The crossover complex slides along the DNA (21, 23), thereby changing the size of the two separated DNA domains. In catenated and knotted DNA, formation of the crossover complex will concentrate some catenane (or knot) nodes in one of the domains. Movement of the enzyme along the DNA contour will eventually trap these nodes in a small loop, thereby facilitating the binding of a T-segment to the topoisomerase (Fig. 4, A and B), which results in strand passage. Because decatenation and unknotting will occur more often when the entrapping DNA loop is small, the effective length of DNA substrate will be shortened and the distribution of topological forms will be simplified. To explain the large magnitude of the effects we observed, we suppose that some additional active mechanism concentrates nodes in the small loop or ensures preferential passage of nodes in the small loop.

The model predicts only a moderate reduction of $\langle \Delta Lk^2 \rangle$ by type II topoisomerases, because for the relaxation reaction, there is no entrapment of the T-segment by the shrinking DNA loop (Fig. 4C). The difference between the steady-state and equilibrium values of $\langle \Delta Lk^2 \rangle$ may result from the formation of domains too small to readily accept writhe (24). The smaller

Fig. 3. Correlation between preferential decatenation, unknotting, and relaxation in topo II catalyzed reactions. The ratio of equilibrium to steady-state fractions of catenanes (R_{cat}), knots (R_{kn}), and the variance of topoisomer distribution (R_{Lk}) is shown for type I (x) and type II topoisomerases (●). The enzymes shown are topoisomerases III (III) and IV (IV) from *E. coli*, the phage T2 topoisomerase (T2), and topois II from *Saccharomyces cerevisiae*, either full-length (Sc) or COOH-terminal truncated (1–1200 aa) (Sc C), *D. melanogaster* (Dm), and human cells (Hs).

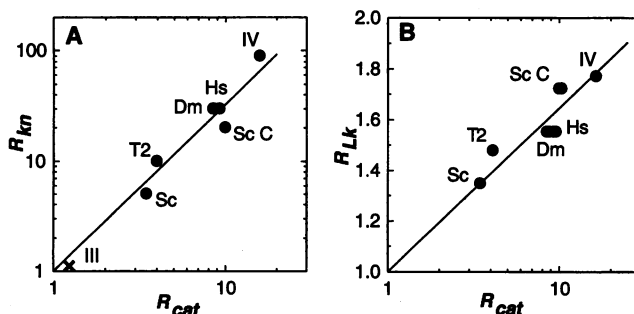
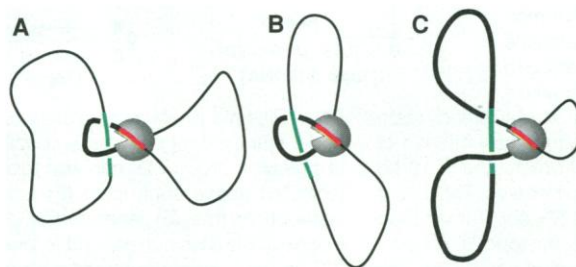


Fig. 4. A three-binding-sites model of type II topoisomerase action. Stable binding of the enzyme to a DNA crossover divides the DNA molecule into two smaller domains, shown by bold and narrow lines. As a result, the local concentration of the T-segment (green) in the vicinity of the enzyme-bound G-segment (red) increases in catenated (A), knotted (B), and supercoiled (C) molecules. In addition, sliding of the protein clamp along the DNA can trap a catenane or knot node in a small loop, thereby facilitating removal of topological links from DNA.



deviation from topological equilibrium for relaxation predicted by the model agrees with our experimental results and provides an explanation for the puzzling observation that type II topoisomerases are much better at decatenation and unknotting than relaxation (10, 13, 14).

The ability of type II topoisomerases to directionally simplify DNA topology is in accord with their physiological role in DNA replication and chromosome segregation (25). Every turn of the double helix that is replicated introduces a positive supercoil or catenane link into topologically constrained DNA, which must be faithfully and rapidly removed by topoisomerases. However, given the high intracellular DNA concentration (26) and the presence of DNA condensing agents, the topoisomerases might instead be expected to ensnarl chromosomes (27). Our discovery that type II topoisomerases untangle DNA molecules against the thermal drive may help solve this problem.

REFERENCES AND NOTES

1. A. D. Bates and A. Maxwell, in *DNA Topology*, D. Rickwood, Ed. (Oxford Univ. Press, New York, 1993).
2. J. C. Wang and N. Davidson, *J. Mol. Biol.* **15**, 111 (1966).
3. V. V. Rybenkov, A. V. Vologodskii, N. R. Cozzarelli, *ibid.* **267**, 312 (1997).
4. R. E. Depew and J. C. Wang, *Proc. Natl. Acad. Sci. U.S.A.* **72**, 4275 (1975).
5. D. E. Pulleyblank, M. Shure, D. Tang, J. Vinograd, H. P. Vosberg, *ibid.*, p. 4280.
6. V. V. Rybenkov, N. R. Cozzarelli, A. V. Vologodskii, *ibid.* **90**, 5307 (1993); S. Y. Shaw and J. C. Wang, *Science* **260**, 533 (1993).
7. J. C. Wang, *Annu. Rev. Biochem.* **65**, 635 (1996).
8. L. F. Liu, C.-C. Liu, B. M. Alberts, *Cell* **19**, 697 (1980).
9. J.-i. Kato, H. Suzuki, H. Ikeda, *J. Biol. Chem.* **267**, 25676 (1992).
10. H. Peng and K. J. Mariani, *ibid.* **268**, 24481 (1993).
11. M. A. Krasnow and N. R. Cozzarelli, *ibid.* **257**, 2687 (1982).
12. To obtain mixtures with twice the equilibrium amount of heterodimeric catenanes, we cyclized P4 DNA (4 $\mu\text{g}/\text{ml}$) in the presence of pAB4 DNA (100 $\mu\text{g}/\text{ml}$). To obtain mixtures with no heterodimeric catenanes, we cyclized P4 DNA in the absence of pAB4. After cyclization, the concentration of DNA substrates in both mixtures was adjusted to 2 $\mu\text{g}/\text{ml}$ for P4 DNA and 50 $\mu\text{g}/\text{ml}$ for pAB4 DNA. The reaction mixtures also contained 20 mM tris-Cl (pH 7.8), 10 mM MgCl₂, 1 mM dithiothreitol, bovine serum albumin (50 $\mu\text{g}/\text{ml}$), 1 mM ATP, and either 80 mM potassium acetate for *E. coli* topoisomerases III and IV and bacteriophage T2 topo II or 200 mM potassium acetate for eukaryotic topo II, so that each enzyme was assayed under its optimal ionic conditions. The reactions were carried out at 30°C for 60 min, quenched by adding 20 mM EDTA, 0.5% SDS, and 100 $\mu\text{g}/\text{ml}$ proteinase K, and incubated for an additional 60 min at 30°C. Because topo III requires single-stranded regions of DNA for optimal activity, this enzyme was assayed on pAB4 DNA containing a 25-nucleotide-long gap generated by exonuclease III from *E. coli*.
13. J. Roca and J. C. Wang, *Genes Cells* **1**, 17 (1996).
14. C. J. Ullsperger and N. R. Cozzarelli, *J. Biol. Chem.* **271**, 31549 (1996).
15. A. V. Vologodskii and N. R. Cozzarelli, *Biophys. J.* **70**, 2548 (1996).
16. Alternatively, topoisomerases could bend DNA upon binding or change its persistence length. This, however, would substantially alter the topological equilibrium only if the enzyme binds DNA every persistence length or so, and the effects we observed were for s values < 1 .
17. Y. S. Vassetzky, Q. Dang, P. Benedetti, S. M. Gasser, *Mol. Cell. Biol.* **14**, 6962 (1994).
18. J. E. Lindsley and J. C. Wang, *J. Biol. Chem.* **268**, 8096 (1993).
19. J. Roca, J. M. Berger, J. C. Wang, *ibid.*, p. 14250.
20. E. L. Zechiedrich and N. Osheroff, *EMBO J.* **9**, 4555 (1990).
21. J. Roca and J. C. Wang, *Cell* **77**, 609 (1994).
22. Roca and Wang found that a large fraction of cross-overs that were bound by the yeast topo II were enzymatically inactive (79). Moreover, in the decatenation of a supercoiled DNA molecule singly linked to an open circle, the enzyme bound preferentially to a G-segment on the supercoiled DNA but efficiently transported a T-segment from the nicked molecule (21). These results suggest that although topoisomerases bind preferentially to a DNA crossover, the T-segment is not ordinarily one of the two crossing segments.
23. N. Osheroff, *J. Biol. Chem.* **261**, 9944 (1986).
24. D. Shore and R. L. Baldwin, *J. Mol. Biol.* **170**, 983 (1983).
25. C. J. Ullsperger, A. V. Vologodskii, N. R. Cozzarelli, *Nucleic Acids Mol. Biol.* **9**, 115 (1995).
26. E. Kellenberger, *Trends Biochem. Sci.* **12**, 105 (1987).
27. W. F. Pohl and G. W. Roberts, *J. Math. Biology* **6**, 383 (1978).
28. We thank T. Hsieh for *D. melanogaster* topo II, K. Mariani for *E. coli* topo III, L. Shen for human topo II, J. Wang for *Saccharomyces cerevisiae* full-length and COOH-terminally truncated topo II, and I. Tinoco, J. Wang, and P. Wolynes for valuable discussions. Supported by NIH grants GM31657 to N.R.C. and GM54215 to A.V.V. and a Howard Hughes Medical Institute Predoctoral Fellowship to C.U.

6 March 1997; accepted 2 June 1997

A Cytoplasmic Inhibitor of the JNK Signal Transduction Pathway

Martin Dickens, Jeffrey S. Rogers, Julie Cavanagh, Art Raitano, Zhengui Xia, Jocelyn R. Halpern, Michael E. Greenberg, Charles L. Sawyers, Roger J. Davis*

The c-Jun amino-terminal kinase (JNK) is a member of the stress-activated group of mitogen-activated protein (MAP) kinases that are implicated in the control of cell growth. A murine cytoplasmic protein that binds specifically to JNK [the JNK interacting protein-1 (JIP-1)] was characterized and cloned. JIP-1 caused cytoplasmic retention of JNK and inhibition of JNK-regulated gene expression. In addition, JIP-1 suppressed the effects of the JNK signaling pathway on cellular proliferation, including transformation by the *Bcr-Abl* oncogene. This analysis identifies JIP-1 as a specific inhibitor of the JNK signal transduction pathway and establishes protein targeting as a mechanism that regulates signaling by stress-activated MAP kinases.

The JNK signal transduction pathway is activated in response to environmental stress and by the engagement of several classes of cell surface receptors, including cytokine receptors, serpentine receptors, and receptor tyrosine kinases (1). Genetic studies of *Drosophila* have demonstrated that JNK is required for early embryonic development (2). In mammalian cells, JNK has been implicated in the immune response (3), oncogenic transformation (4, 5), and apoptosis (6, 7). These effects of JNK are mediated, at least in part, by increased gene expression. Targets of the JNK

signal transduction pathway include the transcription factors c-Jun, activating transcription factor-2 (ATF2), and Elk-1 (1).

Although JNK is located in both the cytoplasm and the nucleus of quiescent cells, activation of JNK is associated with accumulation of JNK in the nucleus (8). Interaction with anchor proteins is one mechanism that may account for the retention of JNK in specific regions of the cell. Anchor proteins participate in the regulation of multiple signal transduction pathways, including the nuclear factor kappa B inhibitor I κ B, the A-kinase anchor protein (AKAP) group of proteins that bind type II cyclic adenosine 3',5'-monophosphate-dependent protein kinase, and the p190 protein that binds Ca²⁺-calmodulin-dependent protein kinase II (9). These anchor proteins localize their tethered partner to specific subcellular compartments or serve to target enzymes to specific substrates (10). Anchor proteins may also create multienzyme signaling complexes, such as the Ste5p MAP

M. Dickens, J. S. Rogers, J. Cavanagh, R. J. Davis, Howard Hughes Medical Institute and Program in Molecular Medicine, Department of Biochemistry and Molecular Biology, University of Massachusetts Medical School, 373 Plantation Street, Worcester, MA 01605, USA.

A. Raitano, J. R. Halpern, C. L. Sawyers, Department of Medicine, University of California School of Medicine, Los Angeles, CA 90095, USA.

Z. Xia and M. E. Greenberg, Division of Neuroscience, Department of Neurology, Children's Hospital, and Department of Neurobiology, Harvard Medical School, Boston, MA 02115, USA.

*To whom correspondence should be addressed.